An Approach to 3-Dimensional Noise Spectral Analysis

Curtis M. Webb

Night Vision & Electronic Sensors Directorate
10225 Burbeck Rd.
Fort Belvoir VA 22060

ABSTRACT

The 3-Dimensional Noise Model developed by D'Agostino and Webb is rapidly becoming the standard metric used to characterize the temporal and spatial noise present in modern day FLIR imagery. This model separates the noise components into seven directionally dependent noise terms. These terms are isolated into spatial and temporal components dependent on their directional characteristics. A value in units of temperature is determined for each component. This approach gives substantial insight into the workings of the sensor and it's nonuniformity correction capabilities. Without knowledge of the spectrum of each of these components though, the impact of each on the Minimum Resolvable Temperature Difference (MRTD) results may be misinterpreted or misconstrued. Knowledge of the spectrum of the 3-D Noise is also imperative when the 3-D Noise model is used as the basis for noise generation in sensor simulation algorithms.

This paper will present a method of obtaining 3-D noise spectrum for each of the seven noise components by first isolating each noise term. Once the individual noise component frames have been isolated, the spectrum of that component will be determined. The determination of the noise spectra of each of the components will then be discussed. Sample 3-D Noise spectrum data will be presented.

0-8194-1823-4/95/$6.00

1.0 INTRODUCTION

The 3-Dimensional Noise model[1] was developed in light of the complex noise terms seen in advanced scanning and staring thermal imagers. The use of advanced detectors, intricate nonuniformity correction schemes and processing have produced complex noises in these types of sensors. These noise components may exhibit directionally dependent characteristics either horizontally, vertically or from frame to frame (time). FLIR92 now takes into account these directionally dependent noise terms in the form of the 7 independent 3-D Noise terms[2]. The addition of these 3-D Noise terms in FLIR92 has made possible more accurate FLIR performance modelling of advanced sensors. The 1975 NVL Static Performance Model[3] used as the primary noise input the standard Noise Equivalent Temperature Difference (NETD). To define the characteristics of that noise a common one-dimensional normalized Noise Voltage Spectral Density (NVSD) analysis was used. Methods for determining NVSD generally centered around the isolation of one of three types of noise; either shot noise, Johnson noise or 1/f noise. Each was generally attributed to the detector or associated amplifier circuitry and combined to produce the overall system NVSD of the common module systems. In any case, the noises included in the NVSD measurement were entirely temporally varying in nature and correlated with the detector scan.

As mentioned above, advanced scanning and staring systems now use complex processing techniques, Time Delay and Integration (TDI) and digital sampling, all in an effort to increase the signal-to-noise ratio. In doing so, the standard detector noises most generally associated with the NVSD measurement have been minimized, but in its place are new types of noises which have become present. These new noises have now been defined in a directionally dependent coordinate system (3-D Noise) in an effort to better understand how each impact the Horizontal and Vertical Minimum Resolvable Temperature Difference and subsequently field performance.

2.0 BACKGROUND

The 3-D Noise model utilizes the averaging in particular directions (horizontal, vertical or frame-to-frame) as a means of isolating and distinguishing each of the seven noise terms defined in the 3-D Noise model. In this paper, the frame or volume isolating and containing only *one* of the seven specific noise terms will be referred to as N_{xyz}, where xyz refers to the direction in which the noise exists (either horizontally (h), vertically (v) or frame to frame (t)). In the standard 3-D Noise nomenclature defined by D'Agostino and Webb, σ_{xyz} indicates the standard deviation of the frame N_{xyz}. For instance, to isolate a frame containing only N_v, the line-to-line nonuniformity noise, the following equation applies:

$$N_v = [D_t D_h (1-D_v)]\{U(t,v,h)\} \qquad \text{eq. 1}$$

where $\{U(t,v,h)\}$ is a 3 dimensional volume or sequence of digital frames containing all types of noise including temporal and spatial.

D_t represents a directional averaging process of the pixels in a sequence of frames from

frame-to-frame (time):

$$Dt\{U(t,[v],[h])\} = \frac{1}{T}\sum_{t=0}^{T-1} U(t,[v],[h]) \qquad \text{eq. 2}$$

D_v represents the directional averaging of the columns (vertical):

$$Dv\{U([t],v,[h])\} = \frac{1}{V}\sum_{v=0}^{V-1} U([t],v,[h]) \qquad \text{eq. 3}$$

D_h represents the directional averaging of the rows (horizontal):

$$Dh\{U([t],[v],h)\} = \frac{1}{H}\sum_{h=0}^{H-1} U([t],[v],h) \qquad \text{eq. 4}$$

Note the terms in brackets, [], represent directions *not* summed over.

The result of the above directional averaging operations (eq. 1) would be a one dimensional array in which each element of that array contains the average intensity of each row or line of the original volume. σ_v would then be calculated as the standard deviation of the array N_v and the result would be divided by the system's reponsivity to yield a value, in units of degrees C, which represents the line-to-line nonuniformity.

Similar procedures are used for the isolation of the remaining six terms.

$$N_{tvh} = [(1\text{-}Dt)(1\text{-}Dv)(1\text{-}Dh)]\{U(t,v,h)\} \qquad \text{eq. 5}$$

$$N_{vh} = [Dt(1\text{-}Dv)(1\text{-}Dh)]\{U(t,v,h)\} \qquad \text{eq. 6}$$

$$N_{tv} = [Dh(1\text{-}Dt)(1\text{-}Dv)]\{U(t,v,h)\} \qquad \text{eq 7}$$

$$N_{th} = [Dv(1\text{-}Dt)(1\text{-}Dh)]\{U(t,v,h)\} \qquad \text{eq. 8}$$

$$N_{h} = [DtDv(1\text{-}Dh)]\{U(t,v,h)\} \qquad \text{eq. 9}$$

$$N_{t} = [DvDh(1\text{-}Dt)]\{U(t,v,h)\} \qquad \text{eq. 10}$$

3.0 THE 3-D NOISE SPECTRUM

In D'Agostino's paper[4] he introduces the nature of the 3-D Noise Power Spectrum. The 3-D Noise Power Spectrum is described in terms of the Wiener spectrum as:

$$\Phi(t', v', h') = \left| \frac{1}{TVH} \sum_{t=0}^{T-1} \sum_{v=0}^{V-1} \sum_{h=0}^{H-1} U(t, v, h)\, e^{-j2\Pi\left(\frac{tt'}{T} + \frac{vv'}{V} + \frac{hh'}{H}\right)} \right|^2 \qquad \text{eq. 11}$$

where t', v' and h' are integer indices attached to discrete locations in the temporal or spatial frequency domain[5].

The above mentioned equation for the 3-D Noise Power Spectrum defines the resulting spectrum as a 3-Dimensional volume (Wiener spectrum) in which two of the three axis are spatial in nature (horizontal and vertical) and the third describing the temporal frequency variations (time or frame-to-frame). In a purely mathematical sense, the equation above (eq. 11) fully describes the frequency nature of the 3-D Noise volume, but due to the complexities which arise in trying to display and analyze the frequency distribution of a 3 dimensional volume, this paper will, instead, break each 3-D noise component up into it's appropriate dimensions using the directional averaging operators described above, and display each 3-D Noise spectrum in seven separate spectrum graphs. The only term which truly exhibits 3-dimensional characteristics is the $\Phi_{t'v'h'}$ (the spectrum of N_{tvh}) which varies in both the horizontal and vertical as-well-as in time (see Figure 1d). The display of the $\Phi_{t'v'h'}$ will be discussed in more detail later. The displaying of the seven noise components into seven power spectra simplifies the analysis of each noise terms as-well-as keeping with the 3-D model adopted by FLIR92.

Figure 1a-d summarizes the partitioning of the 3-D Noise components into it's planer quadrants as described in D'Agostino paper. Figure 1a illustrates the "spatial or t' plane" in which no temporal variations are shown. The areas along the v' and h' axis are one dimensional spectra $\Phi_{v'}$ and $\Phi_{h'}$.

Equations 1 and 5 through 10 isolate each noise using the directional averaging operation described in equations 2-4. Within these isolated frames (N_{tvh}, N_{tv}, N_{th}, N_{vh}, N_v, N_h, N_t) contain only one of the specific 7 components of the 3-D noise volume. For instance, equation 1 isolates a volume containing only the line-to-line noise term, N_v. Within this volume, no noise exists in time (i.e. this is a fixed pattern noise), in addition, no noise exists horizontally. The frame contains only the average intensities of each line, which stays fixed in time. Because the noise exists in only one direction (vertically) and is fixed in time, a one-dimensional spectrum is sufficient to describe this noise term. This is shown in figure 1a as $\Phi_{v'}$ along the v' axis.

Equation 12 details the power spectrum, $\Phi_{v'}$,where N_v is the frame described in equation 1 containing only the average intensities of each line. $\Phi_{v'}$ is a one dimensional power spectrum in which the units along the v' axis are in units of cycles/milliradian.

$$\Phi(v') = \left| \frac{1}{V} \sum_{v=0}^{V-1} (N_v)\, e^{-j2\Pi\left(\frac{vv'}{V}\right)} \right|^2 \qquad \text{eq. 12}$$

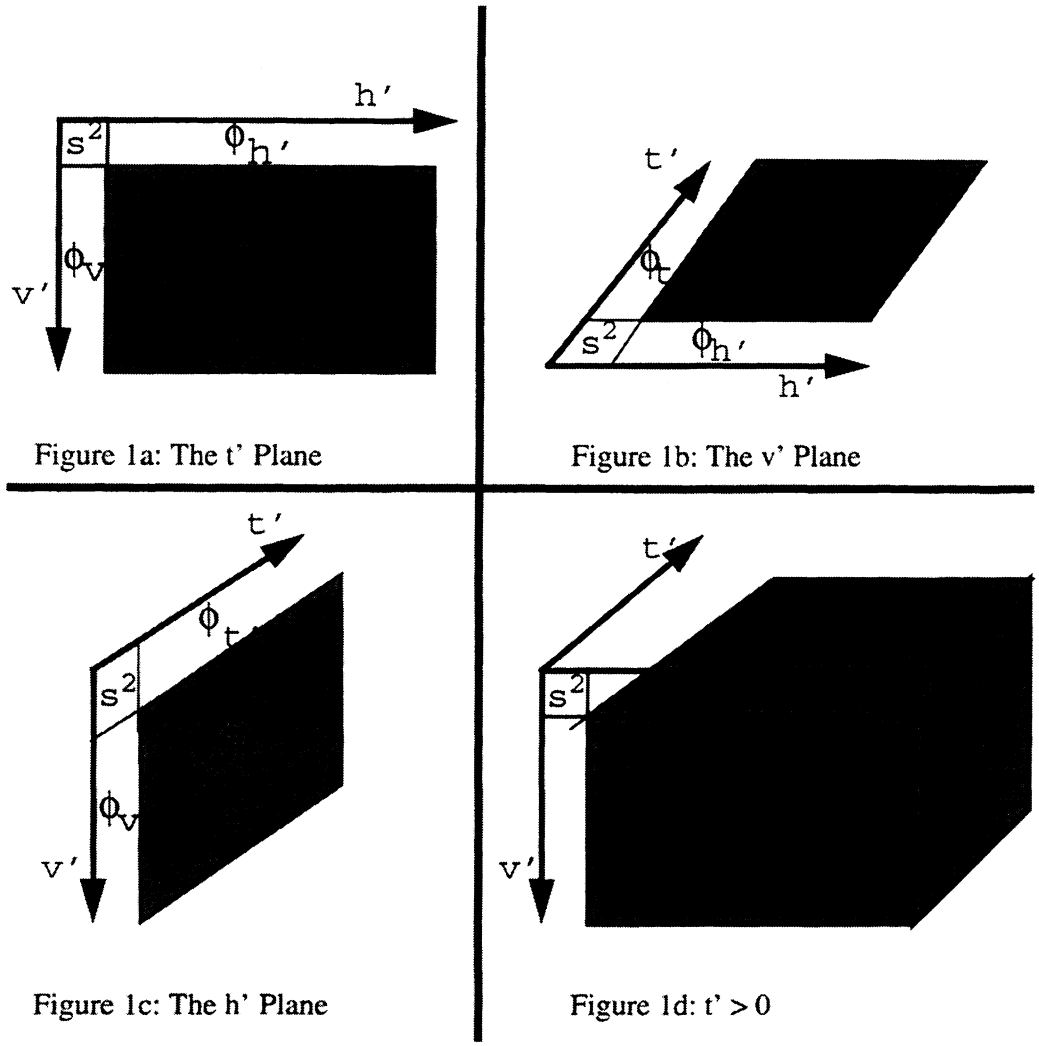

Figure 1a: The t' Plane

Figure 1b: The v' Plane

Figure 1c: The h' Plane

Figure 1d: t' > 0

$\Phi_{v'h'}$, shown in figure 1a, illustrates the 2-dimensional frequency plane which contains the 2-D power spectrum of the image N_{vh}. Once again, this is the power spectrum of the random spatial noise. Equation 13 details the mathematical representation for determining $\Phi_{v'h'}$. N_{vh} is the resulting frame from the process described in equation 6.

$$\Phi(v'h') = \left| \frac{1}{VH} \sum_{v=0}^{V-1} \sum_{h=0}^{H-1} (N_{vh})\, e^{-j2\pi\left(\frac{vv'}{V} + \frac{hh'}{H}\right)} \right|^2 \qquad \text{eq. 13}$$

Similar spectral analysis can be done for the t'v' and t'h' planes as-well-as the one dimensional spectrum for t' (figure 1b and 1c).

Perhaps the most complicated noise spectrum to determine and analyze is that for the noise volume N_{tvh}. This is the noise which varies in all directions (horizontal, vertical and temporal).

Unfortunately, the display and analysis of a complete three dimensional power spectrum is anything but easy. The approach taken here, to simplify the analysis of the 3-dimensional volume of N_{tvh}, is two fold. The first step is that described in equation 14. This equation determines the 2-D power spectrum of each frame in the N_{tvh} volume. Then the average of the power spectra, in the frequency domain, is determined for all the frames.

The power spectrum for $\Phi_{t'V'H'}$ would be calculated as:

$$\Phi(t'V'H') = \frac{1}{T}\sum_{t=0}^{T-1}\left|\frac{1}{VH}\sum_{v=0}^{V-1}\sum_{h=0}^{H-1} N_{tvh}e^{-j2\Pi\left(\frac{tt'}{T}+\frac{vv'}{V}+\frac{hh'}{H}\right)}\right|^2 \qquad \text{eq. 14}$$

where N_{tvh} is defined in equation 5.

The secondary step to the analysis of the power spectrum of the volume N_{tvh} highlights the temporal noise power of each individual pixel (defined here as $\Phi_{T'v'h'}$). Equation 15 describes the formula for determining the average power spectrum of the detectors in a staring array sensor. From the image volume N_{tvh}, the analysis of the power spectrum of each individual pixel/detector is analyzed over the range of frames to obtain the noise power spectrum of each detector. Then, the average noise power of all the detectors is obtained. This particular analysis is most appropriate for staring array sensors in which the detector noise is correlated in time (frame to frame).

Staring Sensor Case

$$\Phi(T'v'h'_{staring}) = \frac{1}{VH}\sum_{v=0}^{V-1}\sum_{h=0}^{H-1}\left|\frac{1}{T}\sum_{t=0}^{T-1} N_{tvh}e^{-j2\Pi\left(\frac{tt'}{T}\right)}\right|^2 \qquad \text{eq. 15}$$

For scanning sensors it is more appropriate to analyze the continuous spectrum along the axis in which the noise is correlated. For a horizontally scanned sensor, the direction of choice would be horizontally. In this way, the actual frequency spectrum of the detectors is determined. Equation 16 details the second step for the determination of the power spectrum for a horizontally scanned array of the noise sequence N_{tvh}.

Scanning Sensor Case

$$\Phi(T'v'h'_{scanning}) = \frac{1}{V}\sum_{v=0}^{V-1}\left|\frac{1}{TT}\sum_{t=0}^{TT-1} N_{tvh}e^{-j2\Pi\left(\frac{tt'}{TT}\right)}\right|^2 \qquad \text{eq. 16}$$

where TT=H*T

Note: for this analysis only, time (TT) is depicted across the horizontal dimension and continuing from frame to frame for a detector scanned horizontally.

For this analysis of a scanning sensor only, as defined in equation 16, the horizontal direction is depicted as time, as is frame to frame. This is necessary because, generally, for a scanning system, the array is one-dimensional. The vertical direction is made up of discrete detectors which are scanned in time along the horizontal direction to make a frame. In the previous discussions, the time aspect in the horizontal scan direction has been ignored in order to simplify the 3-D noise analysis. For this particular analysis of the detector noise power, time actually exists along the horizontal line due to the scanning nature of the system. It is assumed that the last pixel of a line in a particular frame and the first pixel of that line in the next frame are correlated and separated in time by one pixel clock.

Figure 2 illustrates the concept used for the determination of the two components of the noise frame N_{tvh}.

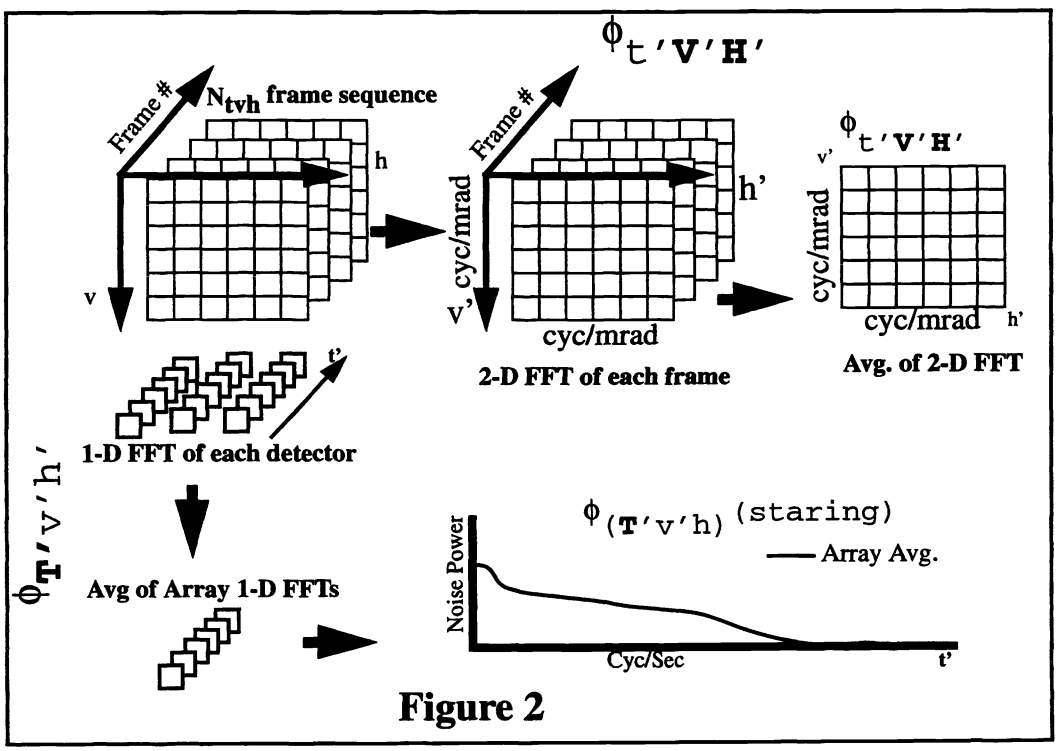

Figure 2

4.0 DATA ANALYSIS AND RESULTS

The following shows results of 3-D Noise analysis and 3-D spectral analysis of a 256*256 staring array infrared camera along with an analysis of the impact of the noise components on the horizontal and vertical MRTD of the system. The system to be analyzed is a 256*256 element staring array with Nyquist frequency cutoffs in both the horizontal and vertical dimensions at 0.7 cyc/mrad. The system operated with a 30Hz frame rate.

Table 1 shows the analysis of the sigma values for the 7 noise terms. These are the standard deviations of the frames describe in equations 5 through 10 reported in units of degrees C[6]. From this

table, it can be seen that there are three dominant terms which contribute to the majority of the noise in the system (σ_{tvh}, σ_{vh} and σ_h). Figure 3 shows the results of the horizontal and vertical Minimum Resolvable Temperature Difference (MRTD). The MRTD curves shown in Figure 3 illustrate some unique phenomena which, in itself, cannot be explained fully with just the 3-D noise results of Table 1. It can be easily explained that the poorer performance seen in the HMRTD curve, as compared to the VMRTD curve, is due to a higher horizontal fixed pattern noise (σ_h or column to column noise). The only other thing that can be surmised by the analysis of the sigma values of the 3-D noise in Table 1 and the MRTD curves is that the random noise terms (σ_{tvh} and σ_{vh}) are a substantial contributor to the noise and it is assumed that they are impacting both the HMRTD and VMRTD equally. For this system, it is clear that a general analysis of just the sigma values of the 3-D noise terms is insufficient to fully describe the impact of the noise on the MRTD results.

Table 1:

	Random	Vertical	Horizontal	Frame
Temporal	σ_{tvh}=0.156	σ_{tv}=0.013	σ_{th}=0.013	σ_t=0.001
Spatial	σ_{vh}=0.108	σ_v=0.012	σ_h=0.129	S=73.753

Figure 4 through 9 shows the 3-D log power spectrum of the frames used to obtain the sigma values shown in Table 1. It should be noted that for each figure the contrast of the spectrum images have been enhanced to enable viewing. Figure 4 shows the 2-D power spectrum, $\Phi_{v'h'}$. This is the fixed pattern noise which exists both horizontally and vertically. It is clear from the spectrum that the noise is anything but random in the horizontal direction. A cluster of increased noise power is seen along the h' axis around 0.2 cyc/milliradian with increased noise power seen along that entire axis as compared to the vertical. From the image of $\Phi_{v'h'}$ seen in Figure 4, it is clear why the curve of the HMRTD is higher across the entire range of targets then the VMRTD curve.

Figures 5 and 6 illustrate the one-dimensional plots of $\Phi_{v'}$ and $\Phi_{h'}$,respectively in units of log power. Again, these are the power spectra of the line-to-line and column-to-column fixed pattern noise of the frames N_v and N_h. It is clearly seen from these plots that the spectrum of the noise in the horizontal direction is far greater then that seen in the vertical direction. Of particular interest are the spikes seen in the $\Phi_{h'}$ plot at frequencies near 0.15 cyc/mrad and also at 0.6 cyc/mrad. At both these corresponding frequencies in the HMRTD curve of Figure 3, the MRTD values increase as a result of those specific frequency noises. The sensor exhibited a very distinct column-to-column nonuniformity fixed pattern.

Figures 7 and 8 show the results of the power spectrum $\Phi_{t'v'}$ and $\Phi_{t'h'}$. Both the σ_{tv} and σ_{th} described in table 1 show a relatively low contribution for these terms. It is interesting to note the noise power seen at about 0.3 cyc/mrad on both the $\Phi_{t'v'}$ and $\Phi_{t'h'}$. This is a result of a rolling diagonal pattern which moves throughout the frame. Because it is a diagonal rolling noise, it will show up on all temporal noise power spectrum plots ($\Phi_{t'v'h'}$, $\Phi_{t'v'}$, $\Phi_{t'h'}$). Again, it should be noted that the intensities of these images have been enhanced to facilitate viewing.

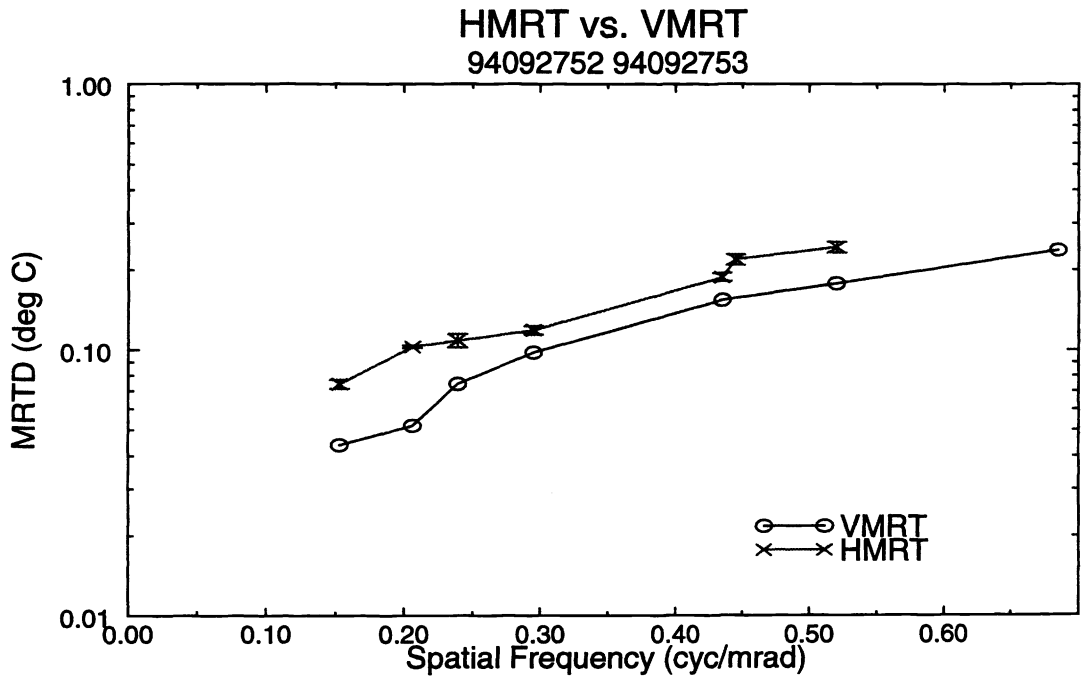

Figure 3

Figures 9a and 9b show the results of the two components of $\Phi_{t'v'h'}$. Figure 9a shows $\Phi_{t'V'H'}$ This is the frequency spectrum of the random temporal noise within a frame in the horizontal and vertical planes. Figure 9b shows the average frequency spectrum of the detectors in the array. The spike seen at roughly 20Hz is the contribution of the rolling diagonal pattern described above.

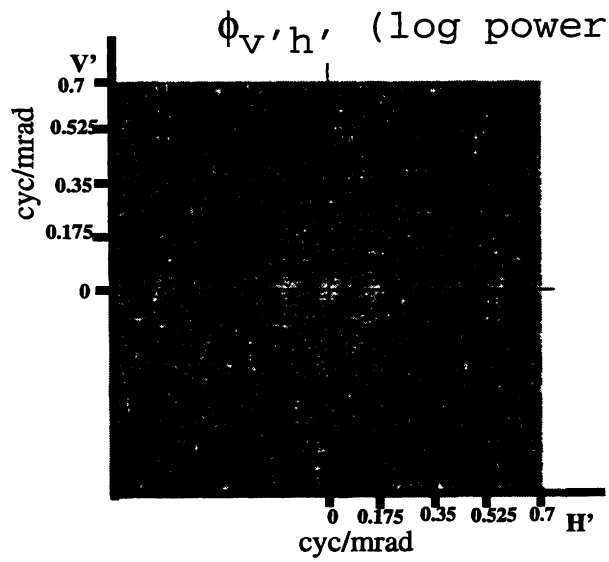

Figure 4

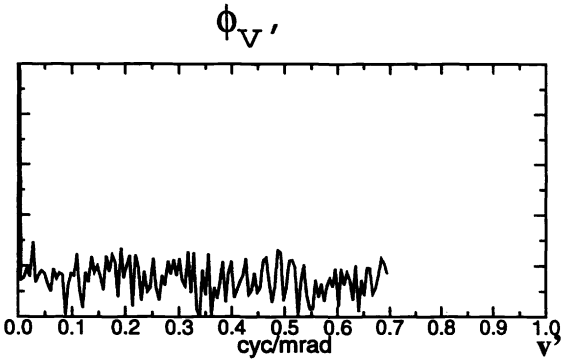

Figure 5

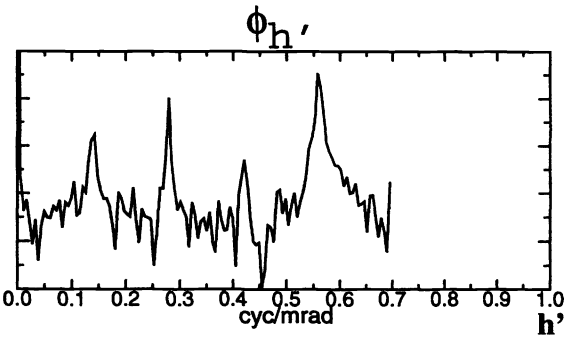

Figure 6

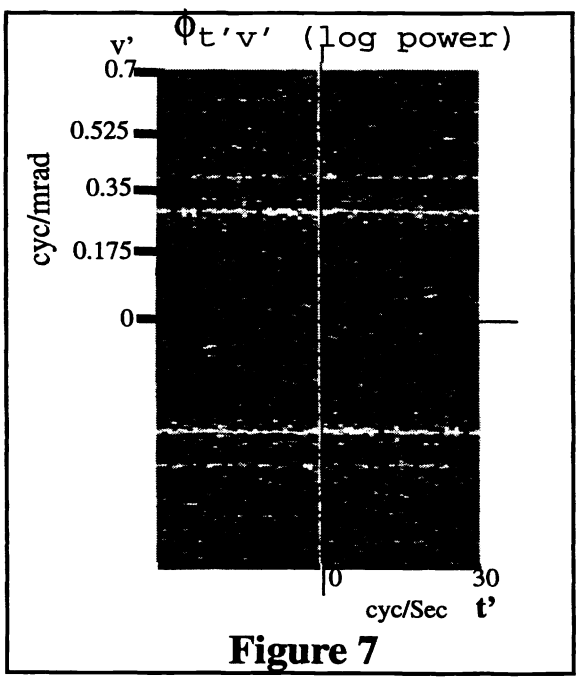

Figure 7

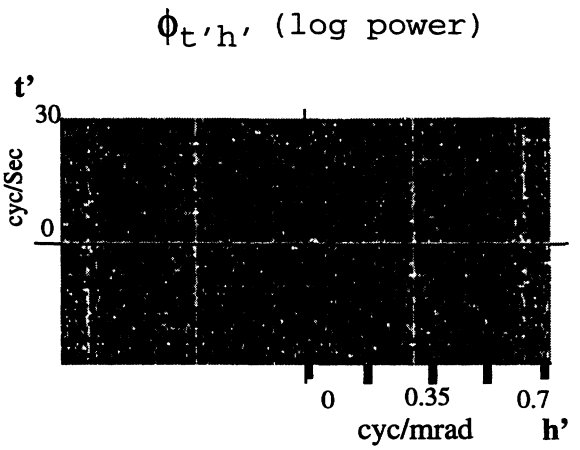

Figure 8

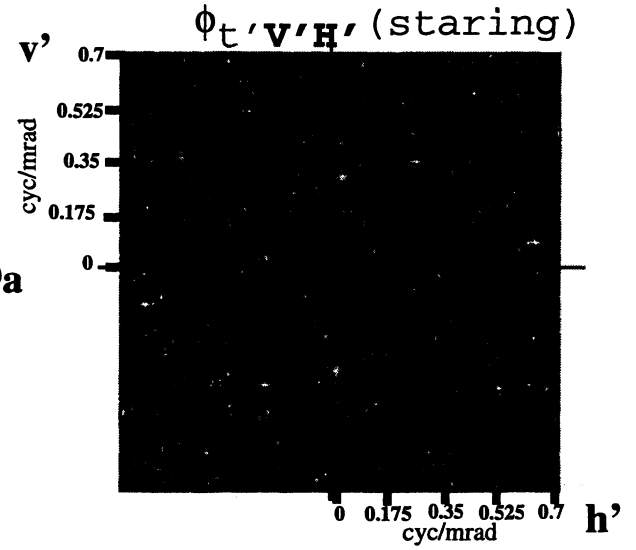

Figure 9a

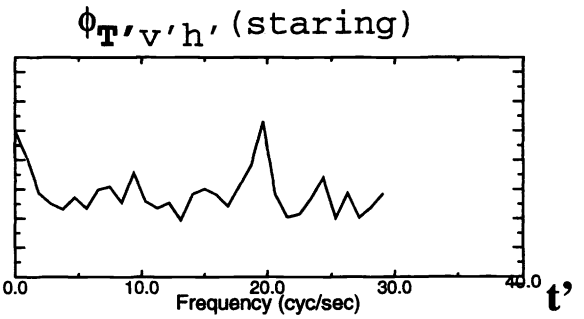

Figure 9b

5.0 MODELING APPLICATIONS

The analysis of the 3-D spectrum allows for the further understanding of the complex noises being generated in advanced sensors. Presently, the standard procedure to determine the sigma values, which are input into FLIR92, use a 2nd order polynomial curve fit to remove very low frequency trends[6]. This was done to remove the low frequency fixed pattern noise which may have a far greater RMS amplitude then the higher frequency noises, but these low frequency trends do little to impact or hurt the MRTD values except at very low frequencies. This trend removal has been a major point of contention among the community as to the impact of removal of noise in the analysis. In addition, historically, FLIR92 has been optimistic in predicting the low frequency MRTD values. It is believed that the inclusion of the 3-D Power Spectrum into FLIR92 would eliminate the need for the trend removal as-well-as improve the low frequency MRTD predictions.

In addition to obtaining a better understanding of the noise for use in sensor modeling, the analysis of the 3-D power spectrum of thermal imagers will also increase the understanding of complex noises for FLIR simulation efforts such as DIS. The complex noise terms can be included in the sensor simulation with accurate representation of the magnitude as-well-as frequency of the noise.

6.0 CONCLUSION

An approach to defining the 3-D Noise Power Spectrum has been presented. This approach, along with the sigma values obtained in the conventional 3-D Noise analysis provides for a better understanding of the noise present in advanced sensors. Sample data has been presented which shows the usefulness of the 3-D Noise Power Spectrum in understanding the impact of the noise on the MRTD measurement.

7.0 REFERENCE

1. D'Agostino J & Webb CM, "Three-dimensional Analysis Framework and Measurement Methodology for Imaging System Noise" Infrared Imaging Systems: Design Analysis, Modeling, and Testing II, GC Holst, Editor, Proc. SPIE 1488, p90.

2. Scott L. & D'Agostino J., "NVEOD FLIR92 Thermal Imaging System Performance Model", Infrared Imaging Systems: Design Analysis, Modeling, and Testing III, GC Holst, Editor, Proc. SPIE 1689, p194.

3.Ratches JA, et al, "Night Vision Laboratory Static Performance Model for Thermal Viewing Systems", April 1975

4. D'Agostino, J, The Modeling of Spatial and Directional Noise in FLIR90, IRIS 1991

5. Gonzalez, RC & Wintz, P., "Digital Image Processing", Addison-Wesley Publishing, 1977

6. Webb CM, et al. "Laboratory Procedure for the Determination of 3-D Noise in Thermal Imaging Systems", IRIS Specialty Group on Passive Sensors, March 1991